17th World Conference on Earthquake Engineering, 17WCEE
Sendai, Japan - September 13th to 18th 2020

IDA-BASED SEISMIC COLLAPSE PATTERNS AND THEIR PREDICTABILITY BY GENERALIZED LINEAR MODELS

K. T. Tsalouchidis[(1)], N. Bijelić[(2)], C. Adam[(3)], L. Moschen[(4)]

[(1)] *Unit of Applied Mechanics, University of Innsbruck, Innsbruck, Austria, konstantinos.tsalouchidis@uibk.ac.at*
[(2)] *Unit of Applied Mechanics, University of Innsbruck, Innsbruck, Austria, nenad.bijelic@uibk.ac.at*
[(3)] *Unit of Applied Mechanics, University of Innsbruck, Innsbruck, Austria, christoph.adam@uibk.ac.at*
[(4)] *VCE Vienna Consulting Engineers ZT GmbH, Vienna, Austria, moschen@vce.at*

Abstract

The assessment of building collapse risk in earthquake engineering typically involves conducting a large number of non-linear response history analyses using earthquake ground motions as excitation for the building models. These analyses are computationally demanding and potentially become infeasible as the number of required analyses increases, as is the case with regional risk assessment of building portfolios. In search of alternative solutions that provide reliable collapse risk estimates with reasonable computational time, this paper examines the efficiency and accuracy of simple machine learning tools, such as linear regression and logistic regression, for predicting collapse intensity. For the development and testing of machine learning algorithms, a structural response database is developed for a well-documented flexible steel frame structure by conducting extensive incremental dynamic analyses (IDA), employing a total of 17,141 earthquake records extracted from the Peer NGA-West2 ground motion database. The analyses show that the patterns of collapse capacities measured in terms of the spectral acceleration at the fundamental period differ significantly depending on the magnitude of the causal earthquakes. Regularized regression is employed for feature selection in which the contribution of a variety of intensity measures to the prediction of collapse is thoroughly examined. The identified features that contribute the most in the accuracy of the collapse predictions are consistent with the outcomes of related work in the literature. The accuracy of the regression models is tested on seven different ground motion subsets with different number of records and corresponding collapse fragilities. The comparison with IDA data shows that the models reliably predict collapse and are therefore suitable candidates for rapid collapse assessment. In the present study, linear regression performs better than logistic regression.

Keywords: collapse prediction, earthquake response, intensity measure, machine learning, regression model

1. Introduction

Quantifying seismic collapse risk is very meaningful from the aspect of performance-based design for safety and resilience. However, required analyses are typically numerically very expensive as they involve multiple evaluations of the limit state function by conducting nonlinear response history analyses. Numerical expense is particularly cumbersome for complex structural models or in regional risk assessments for portfolios of structures. This paper examines simple but effective machine learning approaches for efficient collapse risk estimation.

The use of surrogate models in earthquake engineering is not new, and previous studies have examined demand prediction methods that sidestep the use of response history analyses by leveraging statistical or machine learning tools [1 – 3]. For instance, studies [4, 5] investigated seismogram features that control collapse response of tall buildings and developed efficient and reliable collapse classification algorithms. These analyses utilized the wealth of seismogram data afforded by physics-based ground motion simulations and the developed collapse classifiers were applied to study collapse risk in Southern California. Similar tools are applied in this paper, but the analyses are based on an extensive dataset of recorded ground motions.

With the broader goal of advancing the implementation of machine learning tools in performance-based earthquake engineering to streamline design and allow for rapid risk assessment, this paper examines the suitability of using generalized linear models for seismic collapse response prediction. To enable training of statistical models, a large structural response database is developed by performing incremental dynamic analyses (IDA) [6] of an archetype 12-story steel structure using majority of ground motions from the PEER NGA-West2 database [7]. This dataset yields insights into previously unobserved patterns of collapse response for different seismological features of ground motions. Regularized regression is used as the primary tool to study the utility of different intensity measures for collapse prediction including spectral accelerations, significant durations and sustained amplitude of the ground motion. Finally, regression and classification models are trained and tested for estimation of collapse risk providing insight into the level of accuracy that they can achieve. Opportunities for future work are discussed.

2. Case study building and structural response database

2.1 Building model

A 12-story steel moment frame structure (Fig. 1) is used as a case study building. The building is designed in accordance with [8 – 10] and is analytically described in NIST GCR 10-917-8 [11] (with the archetype ID number "5RSA"). The plan view in Fig. 1 (a) is identical for all stories, with the blue showing the tributary area for gravity loads applied directly to the frame and the green showing the one for gravity loads affecting only the lateral behavior of the frame. To account for the influence of the indirect loads in the modal properties and the P-Delta phenomena, the corresponding masses are applied on an axially rigid leaning column with zero flexural stiffness placed in parallel to the frame (Fig. 1 (b)). The 2D structural model is implemented in OpenSees [12], where the masses representing the loads are lumped and the nonlinear behavior of the members is modelled according to the concentrated plasticity approach with two nonlinear springs at the ends of each element (Fig. 1 (b)). The moment-rotation properties of the plastic hinges follow the modified Ibarra-Medina-Krawinkler model [13, 14] with bilinear hysteretic response. The three fundamental periods of the structure are T_1=3.2s, T_2=1.1s and T_3=0.7s. As such, this is a fairly flexible structure where both higher modes and P-delta effects influence the response.

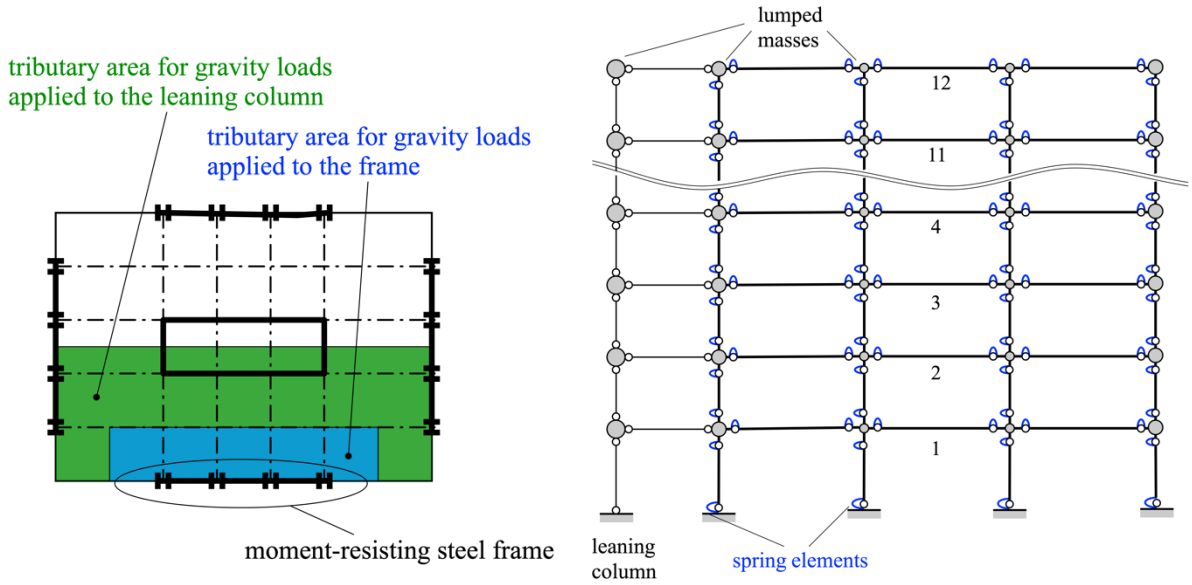

Fig. 1 – Case study building: (a) Typical plan configuration, (b) 12-story frame model (modified from [15])

2.2 Structural response database

To obtain the data for training and testing of machine learning algorithms, we perform IDA for the case study building using majority of the ground motions from the PEER NGA-West2 database. Specifically, we analyze 17,141 ground motions requiring a total of 362,961 nonlinear response history analyses and approximately 10,000 CPU hours of computation time. The database contains information regarding the transient story drift ratios, transient floor displacements and accelerations, of all stories and floors of the frame, at each point in time during the response where a peak value of any story / floor occurred for drifts or displacements and accelerations, respectively, along with the point in time itself. Additionally, the residual values of all these responses are included. The reasoning behind this selection of data is the ability to show the sequence of the entire structure's behavior during the time history, at the time instances when the peak responses of each story and floor occurred. Additionally, the scale factor of the ground motion for each analysis and an indication whether it induced collapse is stored (Table 1). Collapse is considered here as the exceedance of the interstory drift ratio threshold of 10% or dynamic instability and non-convergence of the structural model. In this paper, we limit our attention to collapse responses although other engineering demand parameters (EDPs) are available in our database for future studies.

Table 1 – Structural response database contents

Number of ground motions for IDA	**Total number of response history analyses**	**Available engineering demand parameters (EDPs)**	
17,141	362,961	1. Displacements	Transient EDPs of all stories / floors of the frame at any time instance a peak EDP of each story /floor occurred, as well as residual values.
		2. Drifts	
		3. Accelerations	

3. Generalized linear models (GLMs) for collapse response assessment

The developed structural response database presents a wealth of data to re-examine the question of efficient intensity measures and explore machine learning tools for prediction of collapse response. Moreover, since the response data was obtained using the IDA approach, where each ground motion was successively scaled up to the point of causing collapse, this data can yield insights into issues and effects of excessive scaling of ground motions as well as the influence of different seismological properties of ground motions on the IDA-type collapse process. Before diving into the specifics of the analysis, we first pose structural collapse response estimation as a supervised learning problem involving regression or classification.

3.1 Structural collapse response as a classification or regression problem

In essence, the goal of collapse response estimation is to determine whether a given earthquake ground motion will cause a building to collapse or not. For instance, one can use nonlinear response history analysis to explicitly determine whether a ground motion causes collapse. Alternatively, one can train a statistical model using available collapse response data in order to link the input features of the ground motion (e.g. different intensity measures) to the resulting collapse response (indicated as 1 if the building collapsed under the given ground motion and 0 otherwise). To establish the notation, let $\mathbf{x}_i$ denote the input variables, also called features, and let y_i denote the output variable that is being predicted. A pair $(\mathbf{x}_i, y_i)$ is called a training example, and the dataset of all training examples used to fit or train the model, i.e. a list of m training examples $\{(\mathbf{x}_i, y_i); i = 1, ..., m\}$ is called a training set. Let X denote the space of input values, and Y the space of output values. Then, the goal of supervised learning is, given a training set, to learn a function $h : X \rightarrow Y$ so that $h(\mathbf{x})$ is a good predictor for the corresponding value of y. In our application, different ground motion intensity measures (IMs) are used as the input features $\mathbf{x}$, while the output variable y takes on values of 1 or 0 depending on whether a ground motion induces collapse or not. In this sense, collapse response estimation is a binary classification problem. Alternatively, if the objective of the supervised learning method is to predict the value of collapse capacity given a ground motion, where the output variable y is not binary but a real positive number, then collapse response estimation can be viewed as a regression problem.

3.2 Feature selection

Informed by previous research into comprehensive predictors of structural response [16 – 19], the following set of IMs is considered as a starting set of predictive features: 5% damped peak spectral accelerations at the first three modes of the building, $Sa(T_1)$, $Sa(T_2)$, and $Sa(T_3)$; average of the spectral accelerations (Sa_{avg}) over the period range $0.2\ T_1 – 2.5\ T_1$; ratio of spectral accelerations $Sa_{ratio} = Sa(T_1) / Sa_{avg}$; the 5% to 75% significant duration $D_{a,5\text{-}75\%}$; the arias intensity (I_A) and the cumulative absolute velocity (CAV). In addition to peak elastic spectral accelerations, we also consider the spectral values $Sa(T_1)$, $Sa(T_2)$, $Sa(T_3)$ and Sa_{avg} computed from the 80th percentile values of the 5% damped spectral accelerations in order to capture the sustained amplitude of the ground motion (Fig. 2), which was shown to affect collapse in certain instances [20]. Finally, the seismological characteristics of magnitude (M), source to site distance (JB_{dist}) as defined by Joyner and Boore, and the average shear wave velocity in the top 30m ($V_{s,30}$), are also considered yielding the starting set of fifteen predictors.

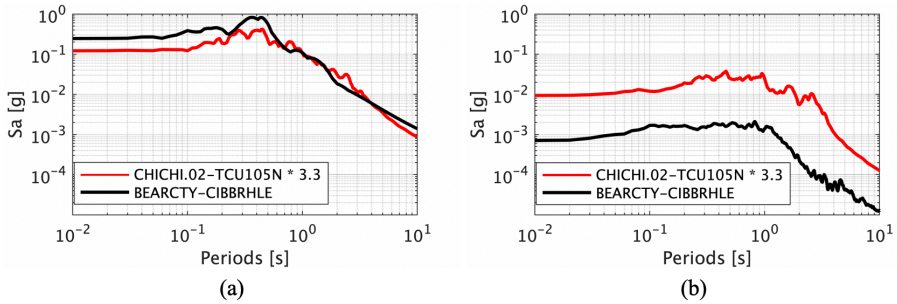

Fig. 2 – Elastic response spectra, Sa: (a) 100th percentile spectrum; (b) 80th percentile response spectrum

Regularized regression is performed to examine which of the above features have the most predictive power for collapse estimation, along with avoiding the pitfall of overfitting the model to the data. Essentially, regularization penalizes the absolute value of regression coefficients θ of the features **x**, resulting in simpler (shrunk) models with less features. For example, in the case of linear regularized regression, the coefficients θ of the model are obtained through the minimization of the equation

$$J = \sum_{i=1}^{m}\left(y_i - \sum_{j=0}^{p}\left(\theta_j \cdot x_{ij}\right)\right)^2 + \lambda \cdot \sum_{j=0}^{p}\left|\theta_j\right| \quad (1)$$

which is the lasso regression [21], where the cost parameter lambda (λ) defines the extent of the penalization on the total of p predictors and consequently the shrinkage of the model.

The results of the regularized regression are presented in Fig. 3 (a) and (b) for the linear and logistic regression, respectively. In these plots, the coefficients of the most important predictors start having non-zero values as the cost parameter is decreasing, indicating a hierarchy in their importance. In both regression schemes, two models are considered, denoted as R1 and R2 for the linear regression and C1, C2 for the logistic regression. Models R1 and C1 include only the two most important predictors, while R2 and C2 include all the features that enhance the models' performance. In Fig. 3 the coefficients' values of these models are indicated by the vertical dotted lines. In the case of linear regression (Fig. 3 (a)), the first two most important predictors are the Sa_{ratio} and the $Sa(T_1)$ (labeled in the figure), which are preserved in the model R1. A more complex model R2 includes the following features: $Sa(T_1)$, $Sa(T_2)$, $Sa(T_3)$, Sa_{avg} (as well as their counterparts computed from the 80th percentile spectra), Sa_{ratio}, $D_{a,5\text{-}75\%}$, M, JB_{dist}, CAV, $V_{s,30}$ and I_A. For the logistic regression (Fig. 3 (b)), the labeled curves correspond to the most important predictors, $Sa(T_1)$ and Sa_{avg} , which are considered in the model C1, while the model C2 includes the $Sa(T_1)$, $Sa(T_2)$, $Sa(T_3)$, Sa_{avg}, their counterparts computed from the 80th percentile spectrum and CAV. The performance of the models R1, R2, C1 and C2 is presented in section 4.

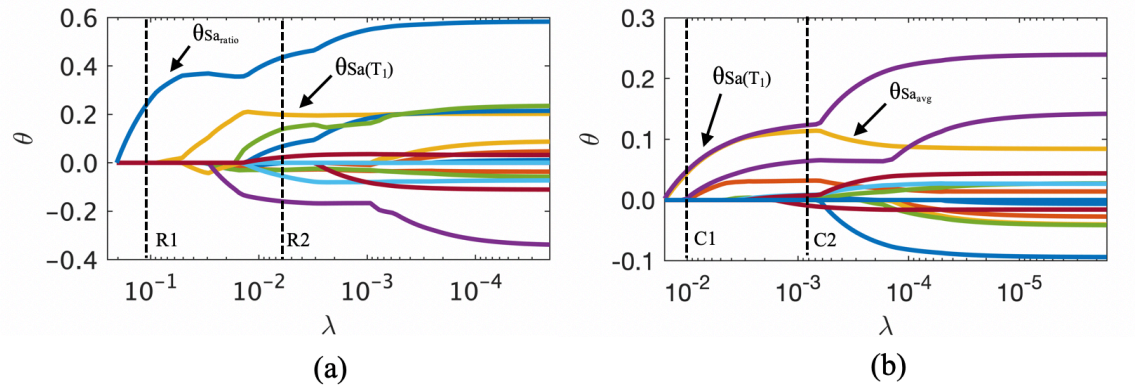

Fig. 3 – Shrinkage of regression coefficients as a function of the cost parameter (λ): (a) linear regression, (b) regularized logistic regression

3.3 Analysis of collapse data

To get a sense of trends in the collapse response data, we perform exploratory data analysis. Fig. 4 shows a scatter plot of collapse capacities of each analyzed ground motion, referred to as $Sa(T_1)$@collapse, as a function of Sa_{ratio} and 5% to 75% significant duration ($D_{a,5\text{-}75\%}$). Sa_{ratio} and $D_{a,5\text{-}75\%}$ are used to represent the data as they were previously observed to correlate well with collapse [22]. This 'arrow-like' shape of the data suggests there are two dominant trends in the data, where a subset of the ground motions exhibits smaller collapse capacities, i.e. these motions are more damaging than the rest of the data with similar Sa_{ratio} and $D_{a,5\text{-}75\%}$. By examining seismological properties of ground motions, a strong dependence on earthquake magnitude M is observed as indicated with points of different color in Fig. 4. Specifically, ground motions from earthquakes

with $M < 6.2$ (blue points) seem to be more damaging than earthquakes with $M > 6.2$. Additionally, it is observed that these damaging records require very large scaling factors (on the order of 100 times and higher) in order to induce collapse of the case study building. This is in contrast to scaling factors of the less damaging motions, which are in the range of 10 to 60.

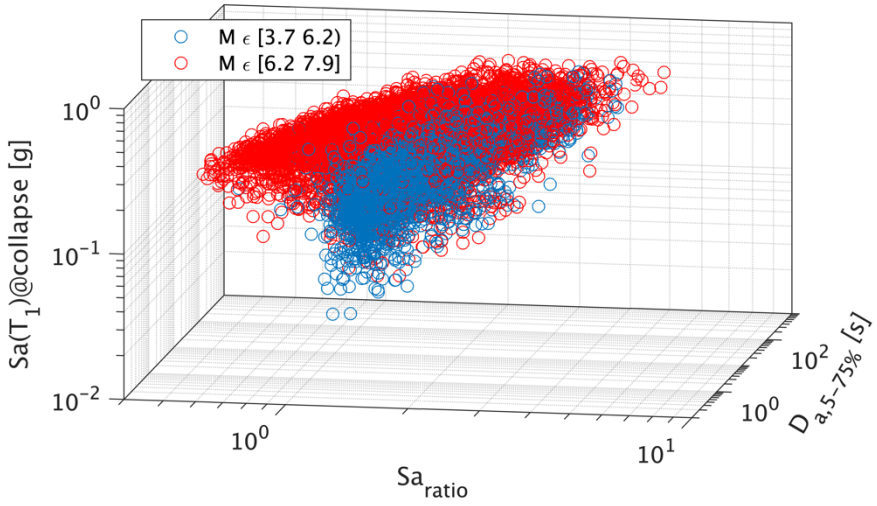

Fig. 4 – Collapse capacities Sa(T1)@collapse as a function of Sa_{ratio} and $D_{a,5\text{-}75\%}$ in log space

To further investigate this collapse trend, we examine the spectra of ground motions from the identified magnitude groups. Fig. 5 (a) shows spectra of ground motions with $M < 6.2$, where the median spectrum is indicated with a thick blue line. These spectra are scaled to have unit value at period T = 3.2s, which is the fundamental period of the case study structure. Fig. 5 (b) shows the corresponding data for ground motions with $M > 6.2$ with the median spectrum indicated in a thick red line. The two medians are contrasted in Fig. 5 (c). It is clear from the median spectra that the records with low magnitudes have significantly higher spectral values at periods T < 3s, which include higher modes of the analyzed building. As a result, these ground motions are comparatively more damaging when using them to conduct an IDA as was observed from their lower collapse intensities (Fig. 4). In subsequent analyses we only use data for ground motions with $M > 6.2$.

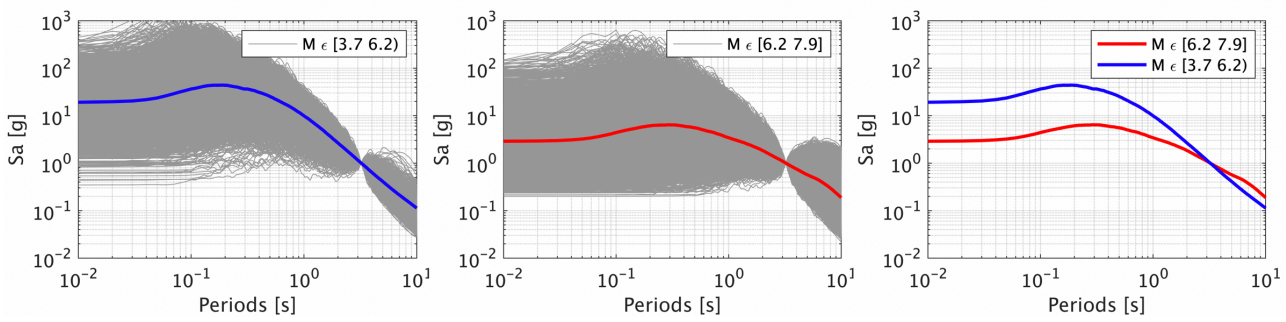

Fig. 5 – (a) individual and median spectra of records with $M < 6.2$, anchored at $Sa(T_1) = 1g$
(b) individual and median spectra of records with $M > 6.2$, anchored at $Sa(T_1) = 1g$
(c) median spectra of records with $M < 6.2$ and $M > 6.2$ obtained from (a) and (b)

4. Assessing the performance of GLMs

After the models have been fitted to the training set, as presented in section 3.1, they must be evaluated in their predictive power (i.e. the ability to output reliable estimates in unseen data – different from the training examples). For this reason, a subset of the database is used as a test set to assess their performance, i.e. the ability of h to output $h(\mathbf{x}_i)$ as a good approximation of y_i, where the training and test sets typically consist of 70% and 30% of the total number of data, respectively.

For the case of logistic regression, since IDA has been performed for every ground motion record, the question is which scales as well as how many analyses from each ground motion should be used as data. In principle, for each ground motion record, every intensity greater than the lowest collapse intensity could be considered as a training example of collapse (y = 1) and equivalently, every intensity lower than the collapse capacity is a training example of non-collapse (y = 0). This issue was investigated, and it was found that no improvement is obtained from considering more data from each IDA than the two analyses that define the boundary of collapse i.e. the collapse capacity and the lowest collapse intensity. Therefore, in the classification problem, two training examples are provided for each record in the training set. On the other hand, in the case of linear regression, the input features x refer to the unscaled record and the output is the collapse intensity $Sa(T_1)@collapse_{predicted}$ and therefore the implementation is more straightforward with one training example per record.

In the following, after the error metric for the assessment of the models is introduced, the models R1, R2, C1 and C2 are evaluated through the test set.

4.1 Error metrics and prediction accuracy

In the case of linear regression, given a ground motion record from the test set with features $\mathbf{x}_i$, the model yields the collapse capacity $h(\mathbf{x}_i) = Sa(T_1)@collapse_{predicted}$, which is compared to the actual collapse capacity $y_i = Sa(T_1)@collapse_{actual}$. The ratio of these values is the following error metric adopted here,

$$error = \frac{Sa(T_i)@collapse_{predicted}}{Sa(T_i)@collapse_{actual}} = \frac{SF@collapse_{predicted}}{SF@collapse_{actual}} \quad (2)$$

which remains the same for any other IM, instead of the $Sa(T_1)$, as long as it is linearly dependent on the scaling of the record (e.g. any other spectral value $Sa(T_i)$ or Sa_{avg}). The values of the error metric on the test set define the accuracy of the model.

In Fig. 6 (a) and (b) the performance of the prediction models R1 and R2 from the linear regression scheme is depicted. The vertical axis shows the predicted intensity $Sa(T_1)@collapse_{predicted}$ while the horizontal axis shows the actual $Sa(T_1)@collapse_{actual}$. Therefore, the slope of the blue lines in this plot corresponds to the error metric from equation (2), because $Sa(T_1)@collapse_{predicted}$ = error * $Sa(T_1)@collapse_{actual}$. In order to assess the performance of the models, the blue lines that are plotted have slopes equal to the 2.5%, 16%, 50%, 84% and 97.5% percentiles of the error metric. Hence, the dashed-dotted lines include the 95% of the test data, the dashed lines include 68% and the solid line corresponds to the median of the error metric. The median values of the models indicate whether they have a bias in their predictions in total (underestimating or overestimating the collapse intensities), and the percentiles indicate how accurate the predictions are. In both models, the median of the errors is approximately 1, which is an indication that both of them perform relatively well on average. As for the accuracy, e.g. in Fig. 6 (b), 68% of the predictions are diverging from the actual collapse intensity by less than 20% (i.e. the error is in the range 0,82 – 1,23). Further insight into the precision of the models is provided in section 4.2. The difference in performance between the models R1 and R2 for the linear regression is evident but not tremendous, underlining the importance of the two main predictors, namely Sa_{ratio} and $Sa(T_1)$, but it also shows the non-trivial contribution of the remaining features.

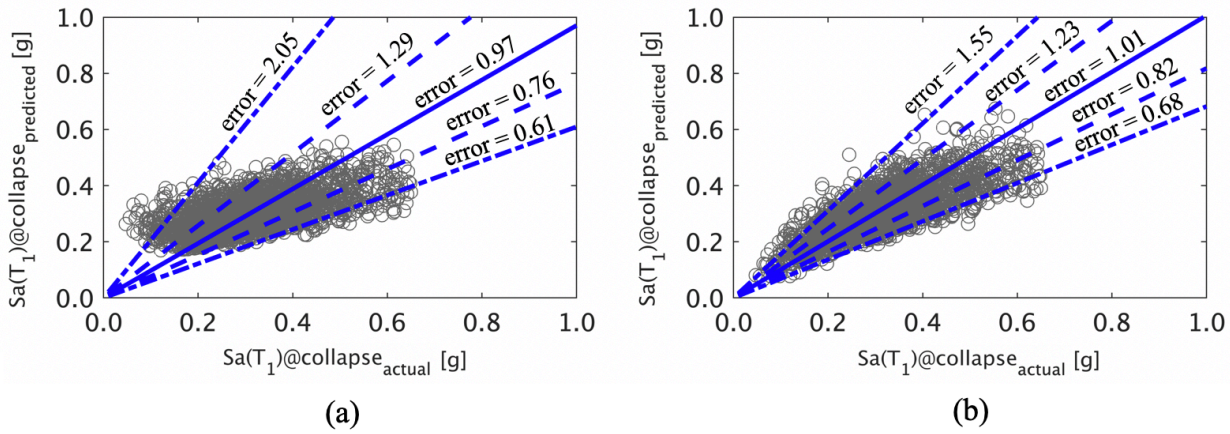

Fig. 6 – Predicted Sa(T_1)@collapse against actual Sa(T_1)@collapse for the linear regression scheme: (a) model R1; (b) model R2

In the case of classification, the testing is not as straightforward, because the model's output $h(x_i)$ is 0 or 1 given the input features (of the scaled record) x_i. The same reasoning as in the training where only the boundary of collapse for each record was used, for the testing of the model we obtain the collapse capacity prediction Sa(T_1)@collapse$_{predicted}$ for each record in the test set as the lowest intensity in which the model outputs $h(x_i) = 1$. This predicted collapse intensity is compared to the Sa(T_1)@collapse$_{actual}$ employing the error metric in equation (2). Fig. 7 shows the results of the models C1 and C2 for the case of logistic regression. The C2 model performs better than C1 in this case, which shows that the features beyond the two main ones should not be neglected as they contribute significantly to the performance of the model.

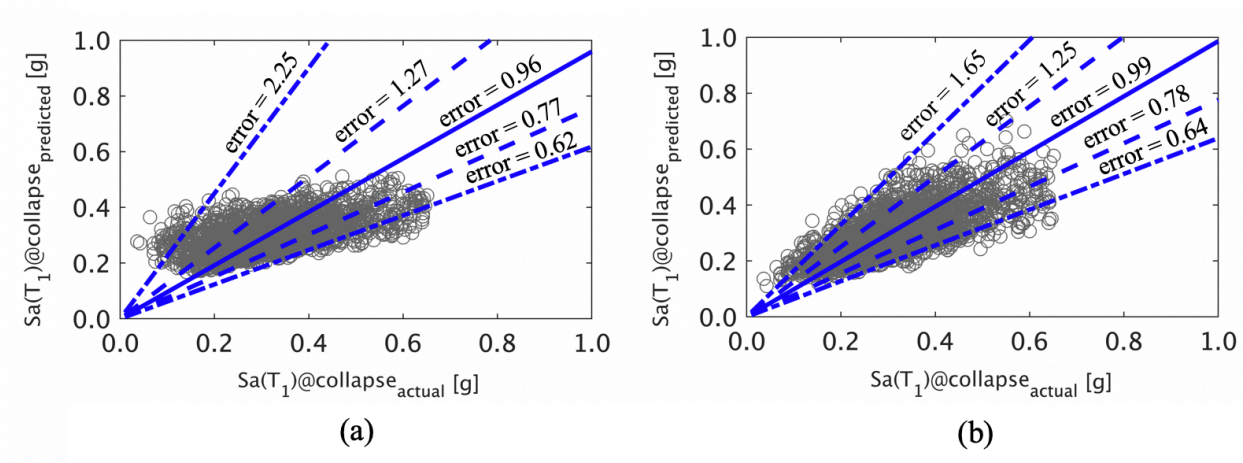

Fig. 7 – Predicted Sa(T_1)@collapse against actual Sa(T_1)@collapse for the logistic regression scheme: (a) model C1; (b) model C2

Comparing the linear regression with the logistic regression schemes for models R2 and C2, we can conclude that the former appears to be more accurate, based on the comparison of the percentile values of the error metric from Fig. 6 (b) and Fig. 7 (b). Moreover, the training, formulation and testing of the model is more straightforward and therefore, in the following, since there is no obvious advantage in performing logistic regression, only the performance of model R2 corresponding to the linear regression is examined.

4.2 Collapse fragilities

To obtain a better understanding of the accuracy of the predictions, the collapse fragilities of several ground motion record sets are computed and are compared with those obtained from the statistical model. The predicted collapse fragility of a ground motion record set used here is the empirical cumulative distribution of the collapse predictions from the regression model, which is compared with the empirical cumulative distribution of the actual collapses obtained from the IDA. In Fig. 8, actual and predicted empirical fragilities are plotted with solid and dashed lines, respectively. Fig. 8 (a) shows the fragilities for the whole test set consisting 2488 records, where the prediction proves to be fairly accurate. In Fig. 8 (b) three subsets out of the test set are extracted, each consisting of 200 records, with distinguishably different fragility functions. These three sets are selected in differing ranges of $Sa(T_1)$@$collapse_{actual}$ in order to assess the model's ability to predict such variations that are diverging from the collapse fragility of the whole test set. Although the predicted fragilities seem to capture these differences adequately, the error is noticeable on the two diverging sets (set A and C), whereas the prediction for the set B is very good. Finally, in order to assess if the predicted fragilities are affected based on the number of records of the sets, Fig. 8(c), Fig. 8(d) and Fig. 8(e) show sets with 20, 100 and 1000 records, respectively. Overall, the predicted and the actual collapse fragilities are in good agreement as can be seen from the medians and standard deviations of the predicted and the actual fragilities for the seven ground motion sets given in Table 2.

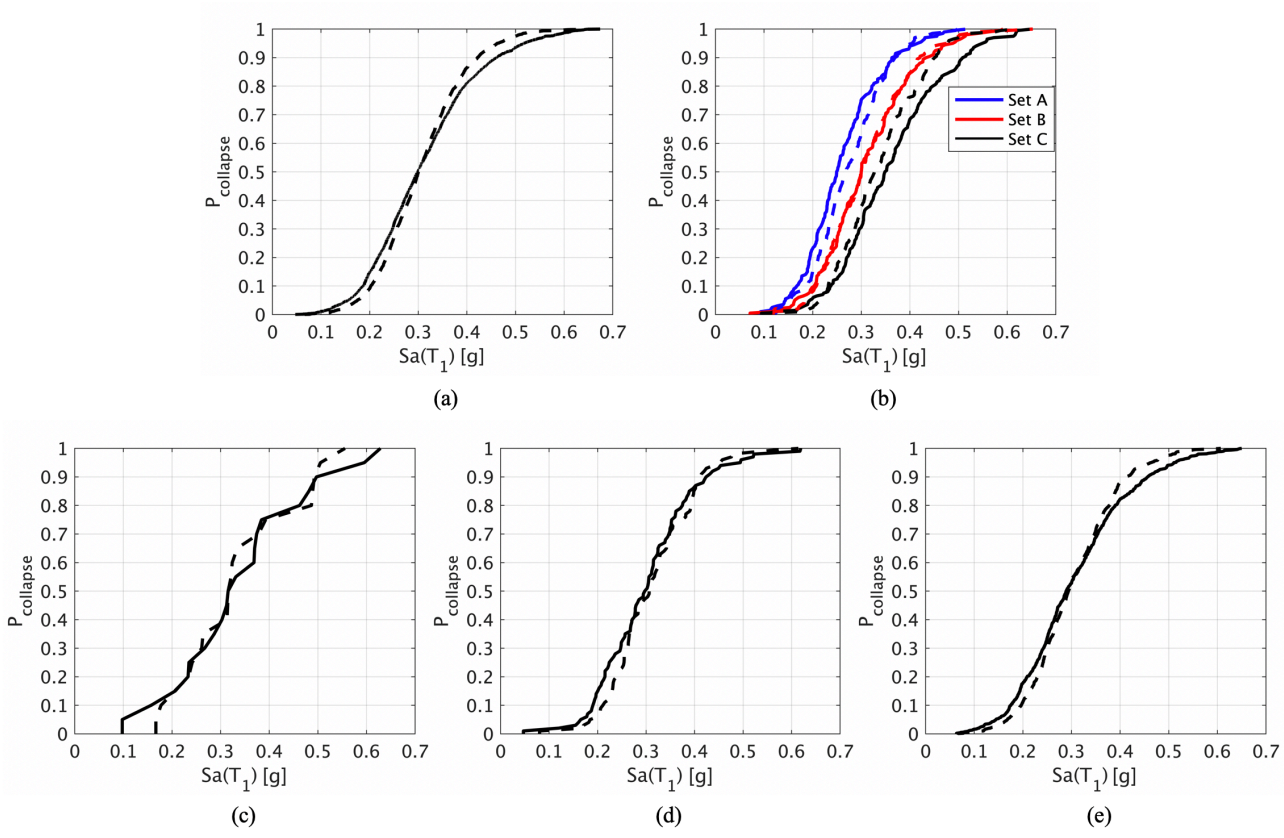

Fig. 8 – Actual (solid lines) and predicted (dashed lines) collapse fragilities: (a) the test set – 2488 records; (b) three sets of 200 records each with significantly different collapse fragilities; (c), (d) and (e) randomly selected record sets containing 20, 100 and 1000 ground motions, respectively

Table 2 – Medians and standard deviations of actual and predicted collapse fragilities

Record set from Fig. 8	Median			Standard deviation		
	Predicted	Actual	Percentage difference	Predicted	Actual	Percentage difference
(a)	0.30	0.30	-0.3%	0.09	0.11	20.0%
(b) – Set A	0.27	0.25	-7.8%	0.07	0.08	7.2%
(b) – Set B	0.30	0.30	0.1%	0.09	0.09	5.5%
(b) – Set C	0.33	0.35	6.5%	0.09	0.11	18.9%
(c)	0.32	0.32	1.4%	0.12	0.14	15.3%
(d)	0.31	0.30	-2.3%	0.09	0.10	14.0%
(e)	0.29	0.29	-1.6%	0.09	0.11	20.2%

5. Conclusions

This study focused on investigating the use of generalized linear models for collapse response prediction based on IDA data. A unique element of the study is the utilization of the greater part of the PEER NGA-West2 database of recorded ground motions, which enables a broad investigation of the mechanisms and parameters that control collapse. Interesting patterns on the level of the collapse intensities as measured in terms of SaT_1@collapse were observed, where the two main clusters of ground motion records appeared to be distinguishable based on the magnitudes of causative earthquakes. Specifically, low magnitude records caused lower collapse intensities and are associated with very large scaling factors in order to cause collapse on the examined frame. Future studies involving pattern recognition in collapse analyses could possibly investigate these trends in more depth, while similar investigations on other structures can shed light regarding the repetition and the extent of these findings.

As the success of the regression schemes depends on solid predictors, a thorough examination of some typically used and recognized intensity measures (IMs), such as the spectral accelerations at the first three periods of the structure and the average spectral acceleration over a period range, along with some more innovative choices, such as the sustained amplitude of the response spectra, was conducted. The already recognized significance of the first period spectral acceleration, the average over a period range and their ratio was confirmed through their importance as predictive features in the models' accuracy. The partial contribution of the percentile values of the response spectra suggests that some collapse mechanisms are under the influence of these sustained amplitudes. A closer examination of the records that were affected by these features and whether specific characteristics can be found among them will enrich the knowledge of the significance of these IMs in the description of these particular ground excitations.

Comparing the linear and logistic regression for collapse prediction shows that the former seems to perform better. To verify the accuracy of the model through the prism of practical application, seven ground motion record sets with different empirical collapse fragilities and number of records were examined. By comparing the actual fragilities as obtained from the IDA analyses with those obtained from the prediction models, it was observed that the regression models are able to capture well the collapse fragilities of the actual results, which makes them promising for extended use in collapse assessments.

6. References

[1] Yazdi AJ, Haukaas T, Yang T, Gardoni P (2016): Multivariate fragility models for earthquake engineering. *Earthquake Spectra*, **32** (1), 441-461.
[2] Koutsourelakis PS (2010): Assessing structural vulnerability against earthquakes using multi-dimensional fragility surfaces: A Bayesian framework. *Probabilistic Engineering Mechanics* **25**, 49-60.
[3] Oh BK, Glisic B, Park SW, Park HS (2020): Neural network-based seismic response prediction model for building structures using artificial earthquakes. *Journal of Sound and Vibration*, **468**, 115109.
[4] Bijelić N, Lin T, Deierlein GG (2020): Efficient intensity measures and machine learning algorithms for collapse prediction of tall buildings informed by SCEC CyberShake ground motion simulations. *Earthquake Spectra* (in print).
[5] Bijelić N, Lin T, Deierlein GG (2019): Classification algorithms for collapse prediction of tall buildings and regional risk estimation utilizing SCEC CyberShake simulations. *13th International Conference on Applications of Statistics and Probability in Civil Engineering*, Seoul, South Korea.
[6] Vamvatsikos D, Cornell CA (2002): Incremental dynamic analysis. *Earthquake Engineering & Structural Dynamics*, **31** (3), 491-514.
[7] PEER (2010): PEER Ground Motion Database. *University of California at Berkeley*.
[8] AISC 358-05 (2005): Prequalified Connections for special and intermediate steel moment frames for seismic applications. *American Institute for Steel Construction*.
[9] AISC 341-05 (2005): Seismic provisions for structural steel buildings. *American Institute for Steel Construction*.
[10] ASCE/SEI 7-05 (2006): Minimum design loads for buildings and other structures. *American Society of Civil Engineers/Structural Engineering Institute.* Reston, VA.
[11] NIST GCR 10-917-8 (2010): Evaluation of the FEMA P-695 methodology for quantification of building seismic performance factors. *National Institute of Standards and Technology*.
[12] McKenna F (2011): OpenSees: A Framework for Earthquake Engineering Simulation. *Computing in Science & Engineering*, **13**, 58-66.
[13] Lignos DG, Krawinkler H (2012): Development and Utilization of Structural Component Databases for Performance-Based Earthquake Engineering. *Journal of Structural Engineering*, **139** (8), 1382.
[14] Ibarra LF, Medina RA, Krawinkler H (2005): Hysteretic models that incorporate strength and stiffness deterioration. *Earthquake Engineering & Structural Dynamics*, **34** (12), 1489-1511.
[15] Gremer N, Adam C, Medina RA, Moschen L (2019): Vertical peak floor accelerations of elastic moment-resisting steel frames. *Bulletin of Earthquake Engineering*,**17**, 3233-3254
[16] Bianchini M, Diotallevi P, Baker JW (2009): Prediction of inelastic structural response using an average of spectral accelerations. *Proceedings of the 10th international conference on structural safety and reliability (ICOSSAR 09)*, Osaka, Japan, 13-19 Sept 2009.
[17] Kohrangi M, Bazzurro P, Vamvatsikos D (2016b): Vector and Scalar IMs in Structural Response Estimation: Part II–Building Demand Assessment. *Earthquake Spectra*, **32** (3), 1525-1543.
[18] Eads L, Miranda E, Lignos DG (2015): Average spectral acceleration as an intensity measure for collapse risk assessment. *Earthquake Engineering & Structural Dynamics*, **44** (12), 2057-2073.
[19] Eads L, Miranda E, Lignos D (2016): Spectral shape metrics and structural collapse potential. *Earthquake Engineering & Structural Dynamics*, **45** (10), 1643-1659.
[20] Bijelić N, Lin T, Deierlein GG (2019): Quantification of the influence of deep basin effects on structural collapse using SCEC CyberShake earthquake ground motion simulations. *Earthquake Spectra*, **35** (4), 1845-1864.
[21] Tibshirani R (1996): Regression Shrinkage and Selection via the Lasso. *Journal of the Royal Statistical Society.* **58** (1), 267-288.
[22] Chandramohan R (2016): Duration of earthquake ground motion: influence on structural collapse risk and integration in design and assessment practice. *PhD Thesis. Stanford University*, Stanford, California, USA.

